

INFLUENCE OF GEOMETRY OF HOLLOW ROLLERS ON THE CONTACT STRESS TO THE LARGE BEARINGS

Sorin Adrian BARABAȘ, Adriana FLORESCU

Transilvania University of Brasov, Romania

Abstract. The research answers to problems appeared in exploitation of large bearings, namely, uneven wear on the rollers and the raceways, as a result of high centrifugal forces. Currently, this problem is solved by execution of a geometric logarithmic profile of rollers which prevents the effects of dangerous contact stresses which occur at the ends of their, profile which requires precision operation with high costs. This paper proposes the use of innovative design of hollow rollers whose profile remains cylindrical and optimization of cavity by finite element analysis performed with Nastran software. The research prove that hollow rollers with different cavities, tested in simulation, reduce inertial masses and have behaviour as good in deformations and much better in contact stress. The geometry of hollow rollers achieved by optimizing the hollow ratio of rollers influences the distribution of contact stress to the ends of roller and provides to the large bearings an increased durability by reducing uneven wear.

Keywords: hollow rollers, elastic contact, ends stress

1. Introduction

In the case of heavy bearings, centrifugal forces takes orders of magnitude close to the loads of the contact surface, sliding velocities becomes large and should be considered in the dynamic analysis of the bearing [1].

The pattern is defined by an inertial system of the rings, an azimuth system (which follow the angular position of the rolling body in relation of position of the inertial system), a system of rolling body and a contact system (for each contact separately). Sliding relations between the roller and inner ring are (Figure1):

$$t = (D_r + r) \cdot \varphi; \quad (1)$$

$$s = r \cdot (\theta + \varphi); \quad (2)$$

$$\delta_e = \frac{t-s}{t} = \frac{(D_r + r) \cdot \varphi - r \cdot (\theta + \varphi)}{(D_r + r) \cdot \varphi}; \quad (3)$$

$$\delta_e = \frac{t-s}{t} = \frac{D_r \cdot \varphi - r \cdot \theta}{(D_r + r) \cdot \varphi}; \quad (4)$$

$$\delta_i = \frac{d \cdot \xi - r \cdot \theta - (d+r) \cdot \varphi}{d \cdot (\xi - \varphi)}, \quad (5)$$

where

t – the movement of a point on the roller measured on the outer and inner ring in a given time interval;

s – the movement of the measured point on the circumference of roller at the same time;

D_r – diameter of rollers disposing;

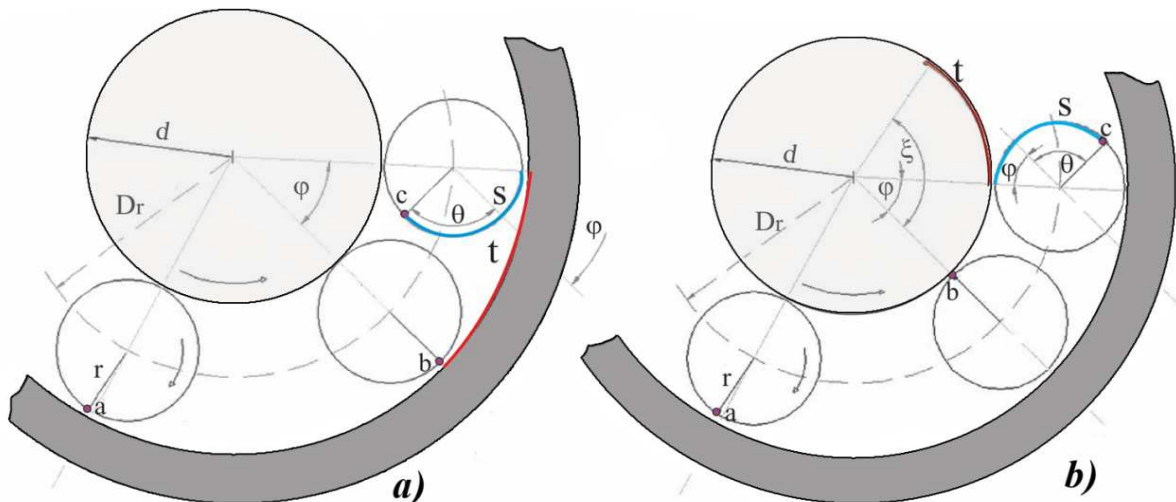


Figure 1. Slidings of the roller bearing
a) on the outer ring b) on the inner ring

φ, ξ – angles between the center of roller in position n and the center of roller in position $n+1$ after a given time interval, as measured on the both, inner and outer raceways [rad];
 θ – a displacement angle of the point of roller in given interval time.

A precise analysis of the bearing must consider contact deformations because they are not equal at all points on the contact surface [2].

Elastic deformations directly influence the size of the angular velocity vector, therefore, influence tangential velocities sizes considered in point of contact and sliding speeds.

Sliding movement produced during working of the bearing has major importance in the emergence of tensions end, the most dangerous for cylindrical roller bearings, increases friction between the roller and ring, generates frictional heat and lead to failure of the system [3].

The rollers can gain additional inclination movements [4] to the axis of the bearing. Relative inclination of the two rings and radial clearance of the bearing rollers have influence over contact stress to the ends of roller.

To the cylindrical rollers with straight ends in the real case of a deformable system, the movement of the contact point and the friction forces are greater than rollers with convex ends.

Therefore, the embodiments will consider this because frictional forces not to lead to major damage to the bearing.

2. The analytical model in the contact area

The used mathematical model was defined by the following equation [5, 6]:

- a) Geometric equation of elastic contact:

$$g(x, y) = h(x, y) - u(x, y) - h_0 \quad (6)$$

expressing the size of the distance between the surfaces after the deformation, as a relationship between the initial separation of $h(x, y)$, carried out in the absence of load, composite deformation $u(x, y)$ and the minimum close h_0 of the bodies, also unknown.

- b) Integral equation of the elastic contact (equation Boussinesq-Flamant):

$$u(x, y) = \frac{2}{\pi} \left(\frac{1-\nu^2}{E} \right) \cdot \iint_A z \cdot d\xi \cdot d\eta, \quad (7)$$

$$z = \frac{P(\xi, \eta)}{(x - \xi)^2 + (y - \eta)^2}; \quad (8)$$

where:

E – Young's modulus;

ν – Poisson's ratio;

$p(x, y)$ – the pressure in the common field;

ξ, η – coordinates on x direction, respectively, y direction, in a tangent plane to the circle of arrangement of rollers.

- c) Equilibrium equation:

$$\int_{A_r} p(x, y) dx dy = Q, \quad (9)$$

where Q is the normal load.

Elastic contact conditions are considered following:

$$h(x, y) = 0; \quad p(x, y) > 0; \quad (x, y \in A); \quad (10)$$

$$h(x, y) > 0; \quad p(x, y) = 0; \quad (x, y \in A). \quad (11)$$

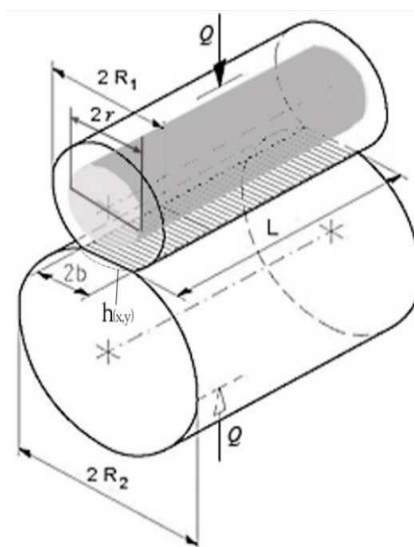


Figure 2. Contact roller-inner ring for hollow rollers

Relative proximity h_0 (Figure 2) in an elastic contact [7] is:

$$h_0 = u_0 + g_0; \quad (12)$$

$$u_0 = \frac{2Q}{\pi \cdot L \cdot E} \left[\ln \left(\frac{2R_1 - 2r}{b} \right) + 0.407 \right]; \quad (13)$$

$$g_0 = \ln \frac{2R_2}{b} + 0.407, \quad (14)$$

where L is the length of the roller, E is Young's modulus, R_1 and R_2 are the radius of the contact bodies (roller and the outer ring), and r is the radius of cavitation.

Using equation (1) can write

$$h(x, y) = h_0 + g(x, y) + u(x, y). \quad (15)$$

Analysis of the two equations (12) and (15) leads to the following conclusion: increasing cavitations makes h_0 to decrease proportionally, resulting in a decrease of $h(x,y)$ thus to lower contact stresses.

Normal force Q can be written as

$$\int_{A_r} p(x,y) \cdot dx \cdot dy = Q = k_1 \cdot \delta^{\frac{10}{9}}, \quad (16)$$

where δ represent moving in the direction of the applied force due to contact and k_1 is a coefficient

that depends on the length of the roller:

$$k_1 = 8.06 \cdot 10^4 \cdot L^{\frac{8}{9}}. \quad (17)$$

Normal radial load force applied to the bearing, generates the compression strain in the roller, which are maximum on generator of roller in contact with the raceways, as well as tensile stress (Figure 3). The arrangement of these tensions is nonlinear.

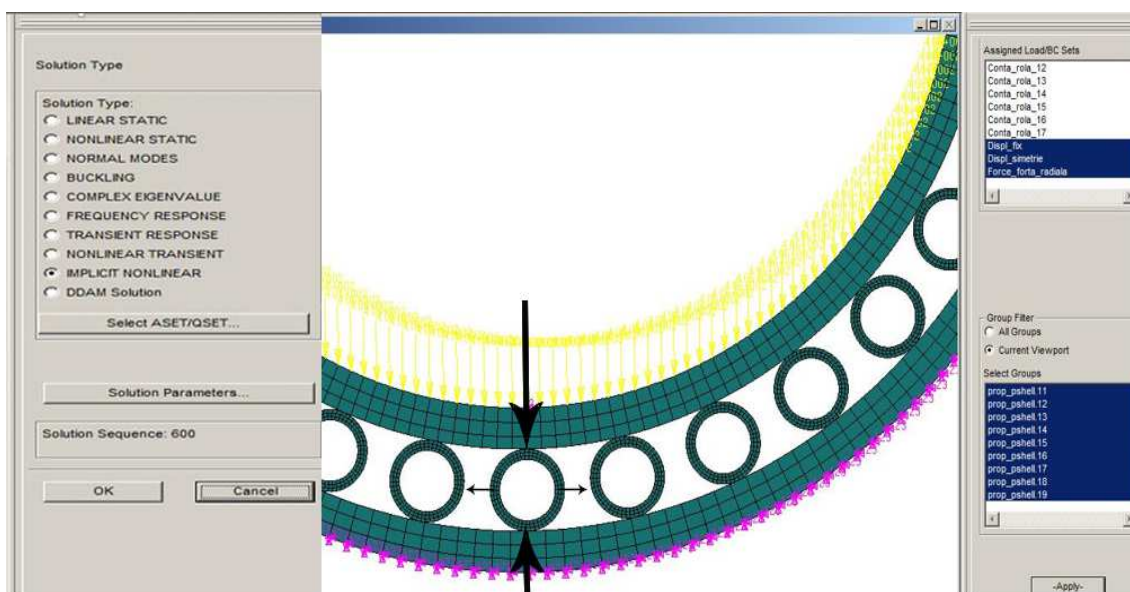


Figure 3. Loads distribution in roller – nonlinear method

3. Results obtained by finite element analysis

In the researches were chosen roller with $D = 120$ mm and $L = 220$ mm from SAE 3310, carburized at 65 HRC. The bearing has the diameter $D_{rul} = 1900$ mm. For the inside diameter (hole diameter) were chosen four cases according to the Table 1.

Table 1. Rollers size analyzed by finite element method

| Cavity diameter D_i [mm] | 0 | 60 | 80 | 90 | 100 |
|----------------------------|-------|-------|-------|-------|-------|
| Roller weight [kg] | 78.22 | 58.67 | 43.46 | 34.22 | 23.90 |

For all four variants were created models in Catia and the analysis was made with Nastran software.

Curve 1 belongs radial cylindrical roller bearing straight and solid (Figure 4). It can be seen that even if the end tensions does not exceed the

permissible limits, bearing wear unevenly, leading to sliding movements. As shown, sliding produces frictions and leading to heat of bearing, fluidization of lubricant, shortening its durability.

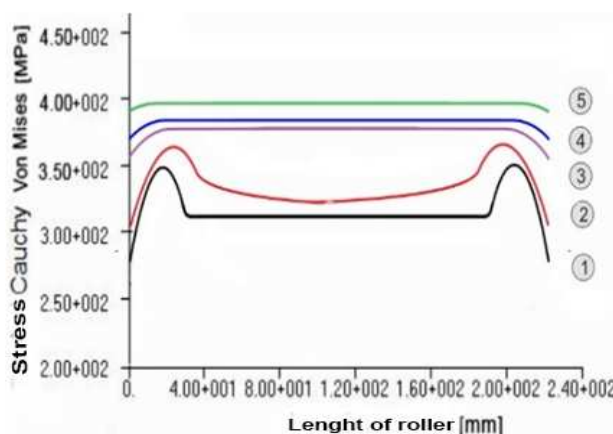


Figure 4. Graph of contact stress in roller depending on cavity-results obtained by finite element analysis

- 1) solid roller $D = 120$ mm; 2) hollow roller $D_i = 60$ mm;
- 3) hollow roller $D_i = 80$ mm; 4) hollow roller $D_i = 90$ mm;
- 5) hollow roller $D_i = 100$ mm

Curve 2 represent a graph of stress contact for hollow roller with $D_i = 60$ mm (Table 1). Respond the requirement to reduce inertial mass in a small measure, without an essential contribution to increasing the efficiency of large bearing assemblies. Both deformations and tensions are similar to the solid roller (Figure 4).

Curve 3 ($D_i = 80$ mm) has end tensions, completely reduced. The bearing has an uniform wear that increases durability. Curve 4 ($D_i = 90$ mm) and curve 5 ($D_i = 100$ mm) have values very close to the curve 3 ($D_i = 80$ mm) were virtually straight profile (stress-free to the end of roller) and respond perfectly to requirements reduction of inertial mass.

4. Conclusions

The reduction of irregular wear is made using hollow rollers. Their degree of cavity increase or decrease masses, forces and inertial and centrifugal moments. Their mounting on large bearing don't present any difficulties. The processing is identical with that of the cylindrical rollers and much more easy and cheap then processing cylindrical rollers with logarithmic profile. Switching to bearing with hollow rollers doesn't require major changes in technology.

The present study is dealing with the problem of their resistance in assemblies bearing – wind power. New problems that the bearing with hollow rollers face, are the bigger deformations and contact stress. The research was conducted taking into account the real radial force from a wind power but the calculations was made on a bearing with cylindrical rollers on one row. In reality this bearing are used rarely, usually bearings on two or four rows. It was considered, in simulation, if a bearing with rollers on a single row responds positive, the results can be extrapolated also on the other type of bearings.

Both the dynamic analysis performed with the help of finite element method as well as the results of the analytical model calculations lead to the conclusion that hollow cylindrical rollers can replace rollers with logarithmic profile, more expensive and heavy, bringing in the same time an increase of life of the bearing through the reduction of uneven wear of rolling elements.

Acknowledgement

This work was partially supported by the strategic grant POSDRU/159/1.5/S/137070 (2014) of the Ministry of Labor, Family and Social Protection, Romania, co-financed by the European Social Fund – Investing in People, within the Sectoral Operational Programme Human Resources Development 2007-2013.

References

1. Liqin, W., Li, C., Dezhi, Z. (2008) *Nonlinear Dynamics Behaviors of a Rotor Roller Bearing System with Radial Clearances and Waviness Considered*. Chinese Journal of Aeronautics, ISSN 1000-9361, vol. 21, no.1, p. 86-96
2. Lai, T.S. (2005) *Geometric design of roller drives with cylindrical meshing elements*. Mechanism and Machine Theory, ISSN 0094-114X, vol. 40, no. 1, p. 55-67
3. Gafițanu, M., Năstase, D., Crețu, Sp., Olaru, D. (1985) *Rulmenți (Bearings)*. Editura Tehnică, București, p. 98-104 Romania (in Romanian)
4. Barabaș, S.A., Șerban, C., Fota, A. (2010) *Reducing the inertial mass of large bearings in wind turbine system using hollow rollers*. Proceedings in Manufacturing Systems ICMA S, ISSN 2067-9238, vol. 5, no. 4, p. 349-352
5. Houpert, L., (2001) *An Engineering Approach to Hertzian Contact Elasticity - Part I*. ASME Journal of Tribology, ISSN 0022-2305, vol. 123, no. 3, p. 582-588
6. Houpert, L., (2001) *An Engineering Approach to Non-Hertzian Contact Elasticity - Part II*. ASME Journal of Tribology, ISSN 0022-2305, vol. 123, no. 3, p. 589-594
7. Kania, L. (2006) *Modelling of rollers in calculation of slewing bearing with the use of finite elements*. Mechanism and Machine Theory, ISSN 0094-114x, vol. 41, no. 11, p. 1359-1376

Received in October 2014